TESTING A LANDSLIDE-GENERATED TSUNAMI MODEL. THE CASE OF THE NICOLET LANDSLIDE (QUÉBEC, CANADA)

GEOQuébec 2015
Challenges from North to South
Des défis du Nord au Sud

Franz, Martin, Jaboyedoff, Michel, Podladchikov, Yury
Institut des Sciences de la Terre, Faculté des Géosciences et de l'Environnement – Université de Lausanne, 1015 Lausanne, Suisse
Locat, Jacques
Laboratoire d'études sur les risques naturels, Département de géologie et de génie géologique – Université Laval, 1065 Laval, Québec, Canada

ABSTRACT
In order to assess comprehensively landslide-triggered tsunamis and the induced risks, we have developed a numerical model which simulates this phenomenon. In order to confirm its capacity to be used as a predictive tool for risk assessment, the model is tested on a real case. The Nicolet landslide (Québec, Canada) occurred on the 8 May 2006 on the Nicolet Sud-Ouest River located in the center of the St-Laurence Lowland. This partially submerged landslide has a volume of about 13'000 m^3. The slide led to a wave and the resulting horizontal run-up distance reached 60 meters on the opposite shore (clearly identifiable on an aerial). The results of our model fit well with the real case, which indicate its ability to simulate such phenomenon and thus confirm its validity.

RÉSUMÉ
Dans le but d'évaluer de manière exhaustive les tsunamis générés par glissement de terrain et les risques associés, nous avons développé un modèle numérique capable de simuler un tel phénomène. Pour confirmer sa capacité à être utilisé comme outil dédié à l'étude du risque, le modèle est testé sur un cas réel. Le glissement Nicolet (Québec, Canada) a eu lieu le 8 mai 2006 au bord de la rivière Nicolet située au centre des basses terres du Saint-Laurent. Ce glissement partiellement submergé a un volume de 13'000 m3. Le glissement a conduit à une vague qui, en débordant, a pénétré de 60 m sur la berge opposée (clairement identifiable sur une photo aérienne). Les résultats obtenus à l'aide de notre modèle correspondent bien avec le cas réel, ce qui prouve sa capacité à simuler un tel phénomène et ce qui confirme sa validité.

1 INTRODUCTION

The landslide-generated tsunami is a phenomenon that threatens infrastructures and lives. In order to assess comprehensively this phenomenon and the induced risks, predictive models are necessary. Currently, three different types of models are used. The first type is theoretical and empirical models often developed from scale models (Slingerland and Voight, 1979; Heller et al., 2009). They are a relevant first approach but are limited in the sense that they cannot fully take into account the bathymetry (Slingerland and Voight, 1979). The second type is 3D models (Ward and Day, 2011). They are the most accurate method to simulate the phenomenon due to the fact that they fully take into account physical parameters and that they use the lesser approximations. On the other hand they require very high computational power. The third type is 2D models (or 2.5D as they are represented in 3D). They are mostly based on Shallow Water Equations (SWE) (Wieczorek et al., 2007; Toro and Garcia-Navarro, 2007; Kremer et al., 2012) and Boussinesq equations (Løvholt et al., 2015). Both of them are approximations of the Navier-Stokes equations. They are less precise than 3D models, but have the great advantage to be usable on standard workstation. We choose to develop a SWE based model because it takes into account precisely the bathymetry; the approximation is considered precise enough; and is affordable in terms of computation power.

Although the SWE method is widely used and accepted, the wet-dry transition, necessary for run-up and flooding simulation, lead to numerical instabilities and remain a main issue (Zijlema and Stelling, 2008).

The goal of this paper is to demonstrate that our model is able to simulate the whole phenomenon of the well-documented Nicolet landslide tsunami.

2 CASE STUDY

The Nicolet landslide (Québec, Canada, Fig.1) occurred on May 8th 2006 on the extrados of a meander of the Nicolet Sud-Ouest River located in the center of the St-Laurence Lowland. The materials are mainly composed of Champlain Sea sensitive clays. This partially submerged landslide has an estimated volume of 13'000 m^3, is 80 m wide and the crest retrogressed up to 15 m (Jaboyedoff et al., 2009).

Figure 1: Location of the Nicolet landslide (modified after Jaboyedoff et al., 2009)

The geometry of the mass before and after the event is particularly precise thanks to an Airborne Laser Scanner (ALS) High Resolution Digital Elevation Model (HRDEM) acquired in 2003 and a Terrestrial Laser Scanner (TLS) point clouds acquired on 11 May 2006 (Minoia and Oppikofer, 2006). During the sliding process the water was pushed by the front of the sliding mass leading to the generation of a wave. The resulting run-out distance up to 60 meters on the opposite shore is clearly identifiable on an aerial photograph taken the May 9th 2006 (Fig. 2). The quality and quantity of data concerning the landslide mass as well as the induced wave run-up make this site a case study of choice.

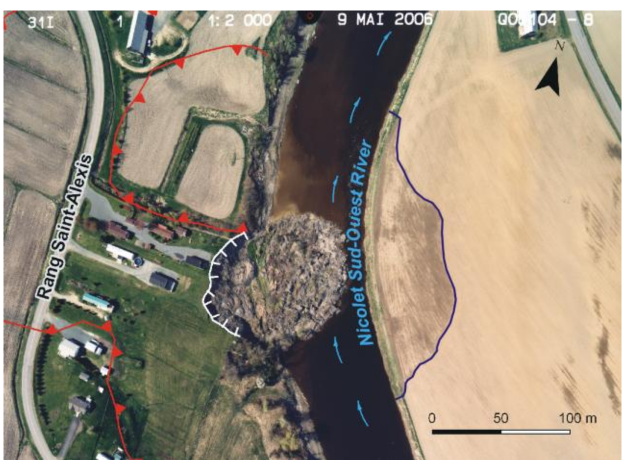

Figure 2. Aerial acquired the 9 May 2006 of the Nicolet landslide. Red lines: former slides scars; White line: limits of the 2006 landslide. The different color on the opposite shore (delimited by the purple line) is the trace of the run-up of the tsunami induced by the landslide (From Jaboyedoff et al., 2009).

The flow of the Nicolet Sud-Ouest River is estimated to be between 20 and 30 m3/s (http://geoegl.msp.gouv.qc.ca/adnv2/tableaux/TableauRegionSimple.php?id=17&type_rapport=ADMIN; https://www.cehq.gouv.qc.ca/suivihydro/graphique.asp?NoStation=030101).

The ALS HRDEM (0.5 m) of the area does not provide information about the bathymetry of the bed of the Nicolet Sud-Ouest River. As the bathymetry is a primordial data for the tsunami simulation, it has to be created.

3 METHODOLOGY

3.1 Bathymetry of the river

The construction of the river bathymetry is performed using the SLBL routine (Jaboyedoff et al., 2004). The river thalweg is assumed to be at 2 masl and located at 2/3 of the width of the river, on the side of the extrados. The thalweg is used as the base level from which the river bed is numerically dug. The subaqueous slopes are built in the continuity of those in the open air.

3.2 Slide

The Landslide mass used for the generation of the tsunami in the model is recreated using the SLBL routine (Jaboyeoff et al., 2004). This step is constrained by the cross-sections from the pre and post failure DEM.

The slide displacement is performed using the viscous flow equations (eq. 8; Turcotte and Schubert, 2002) and is completed apart from the tsunami simulation. The slide displacement and deformation is performed and afterward is implemented as an input in the tsunami model. This step aims to reproduce the displacement including the spreading of the mass, fitting as well as possible the observed deposit. This implies that the behavior of the slide during the event is only reckoned and that it is not properly a model of slide propagation. The velocity of the slide is calculated using the following equation form Heller et al. (2009):

$$V = \sqrt{2g\Delta z_{sc}(1 - \tan\delta \cot\alpha)}\,. \qquad [1]$$

and from Slingerland and Voight (1979) and Wieczoreck et al. (2007):

$$V = V_0 + \sqrt{2gs(\sin\alpha - \tan\delta \cos\alpha)} \qquad [2]$$

Once the velocity calculated, the slide mass undergoes an imposed pace based on it in the tsunami model.

3.3 Tsunami

The tsunami model is based on the two dimensional SWE

$$\frac{\partial U}{\partial t} + \frac{\partial F(U)}{\partial x} + \frac{\partial G(U)}{\partial y} = 0 \qquad [3]$$

where U the solution vector, F and G the flux vectors are defined as

$$U = \begin{bmatrix} h \\ hu \\ hv \end{bmatrix} \quad [4]$$

$$F(U) = \begin{bmatrix} hu \\ hu^2 + \frac{1}{2}gh^2 \\ huv \end{bmatrix}, \qquad G(U) = \begin{bmatrix} hv \\ huv \\ hv^2 + \frac{1}{2}gh^2 \end{bmatrix} \quad [5]$$

where h is the water depth, u and v are the components of the depth averaged velocity vectors, and g is the gravity acceleration. The one-dimensional conservative form is

$$U_i^{n+1} = U_i^n - \frac{\Delta t}{\Delta x}\left[F_{i+\frac{1}{2}} - F_{i-\frac{1}{2}}\right], \quad [6]$$

where $F_{i+1/2}$ is the intercell numerical flux corresponding to the intercell boundary at $x = x_{i+1/2}$ between cells i and i+1. The Lax-Friedrichs numerical scheme defines the intercell flux $F_{i+1/2}$ as follows (Toro, 2001; Franz et al., 2013):

$$F_{i+\frac{1}{2}}^{LF} = \frac{1}{2}\left(F_i^n + F_{i+1}^n\right) + \frac{1}{2}\frac{\Delta x}{\Delta t}\left(U_i^n - U_{i+1}^n\right) \quad [7]$$

The Lax-Friedrichs scheme is regarded as too diffusive (Toro, 2001), but it has been shown that this problem is solved when the model is run with high resolution (Franz et al., 2013).

In order for the model to handle the wet-dry transition, a feature is added to the SWE model. The equivalent to a fine film of water is wrapping the whole topography and its behavior is governed by the following one-dimensional viscous flow model where the flux q for the dimension x is defined by the following equation from Turcotte and Schubert (2002):

$$q_x = -\left(\sin(\alpha_x) + \frac{\partial H}{\partial x}\right)\frac{\rho g H^3}{3\mu} \quad [8]$$

where α is the slope of the topography, H the depth of the film, ρ the density, and µ the viscosity. Where nothing is happening (no wave neither overflowing) the equation 6 is updated with the fluxes obtained with the equation 8 (Viscous Flow). When the wave, thus a certain velocity and a certain thickness, reaches a given point, the equation 4 is updated with the fluxes obtained with the equation 7 (Lax-Friedrichs). The choice of which equation is used is determined by the Reynolds number:

$$Re = \frac{\rho V L}{\mu} \quad [9]$$

where ρ is the density, V the velocity L the depth (or thickness) and µ the viscosity. Over a certain threshold of Re, the flux is determined by the SWE model, and under it, by the viscous flow model. The same principle is applied for the 1D and 2.5D model. For the 2.5D model, the flow of the river is implemented using boundary conditions at 25 m^3/s.

4 RESULTS

4.1 Landslide

For the one dimensional case, the slide mass undergo simultaneously an imposed translation and diffusion. The diffusion increases the length of the sliding mass by 28%. The mean velocity of the front is of 4 m/s. The Fig.3 (center and bottom) shows that the slide at rest (red line) correspond well with the real deposit surface (thin black line) acquired by TLS. It is the displacement of this mass that generates the tsunami.

Concerning the 2.5D case, the SLBL method gives a landslide mass with a volume of 15'600 m^3 and a maximum thickness of 9 m. The original area measures 4500m^2 and spreads to reach an area of 7078 m^2, which represents an increase of 57%. It is noteworthy to mention that this apparently important rise of the surface can be explained by the fact that the numerical propagation leaves a thin layer behind the displaced mass, which is considered in the surface calculation. The instantaneous velocity of the front drops from 10 to 0 m/s in 11 seconds while the mean velocity begin at 10 m/s to eventually reach 4 m/s. The numerical slide displacement and spread match relatively well the observed deposit.

4.2 Tsunami

The results of tsunami simulation performed in 1D and in 2.5D are presented in this section.

4.2.1 1D model

The simulation of the tsunami generation, its propagation and the run-up is presented in Fig.3. It shows that the wave behaves correctly, propagate on the opposite shore (dry to wet transition) and that it reaches a distance of about 70 m away from the initial shoreline, which matches well with the observed distance of propagation of 60 m (Fig. 2).

4.2.2 2.5D model

The 2.5D model simulates the event in a much more complete way. Indeed, the lateral spread of the wave is taken into account but also the flow of the river is implemented in the code. The results presented in the Fig. 4 shows the generation of the wave (top) and the run-up wave propagation on the shore. The simulation doesn't fit perfectly the observed extension (red line). However, the order of magnitude is very similar and the shapes look the same. This result confirms our model.

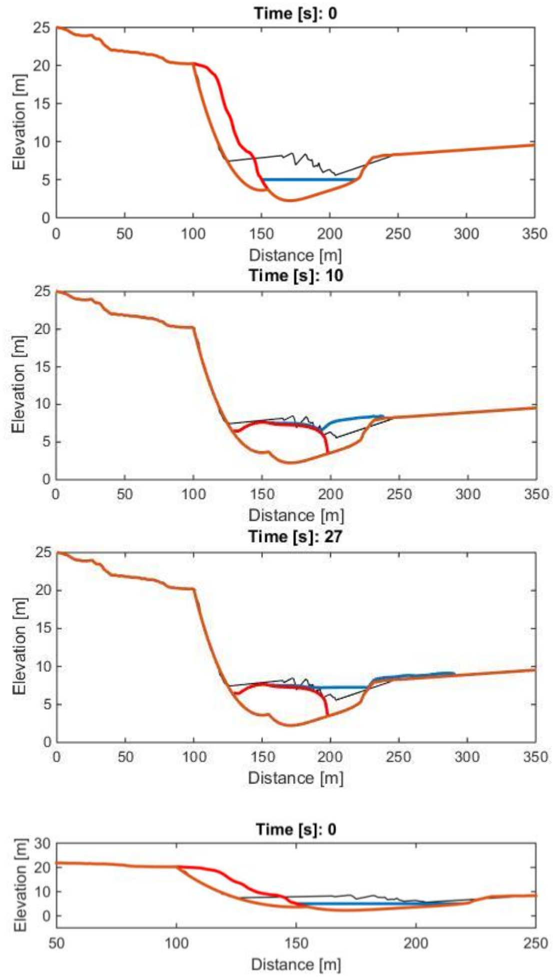

Figure 3. 1D simulation results represented with vertical exaggeration. Brown line: the topography, including the bathymetry and the sliding surface; Red line: the slide mass; Blue line: the water level; Thin black line: the deposit of the slid mass obtained by TLS in 2006. 1: initial situation, 2: the slide is at rest and the wave is generated; 3: the run-up reaches its maximum extension, 4: Cross-section without vertical exaggeration.

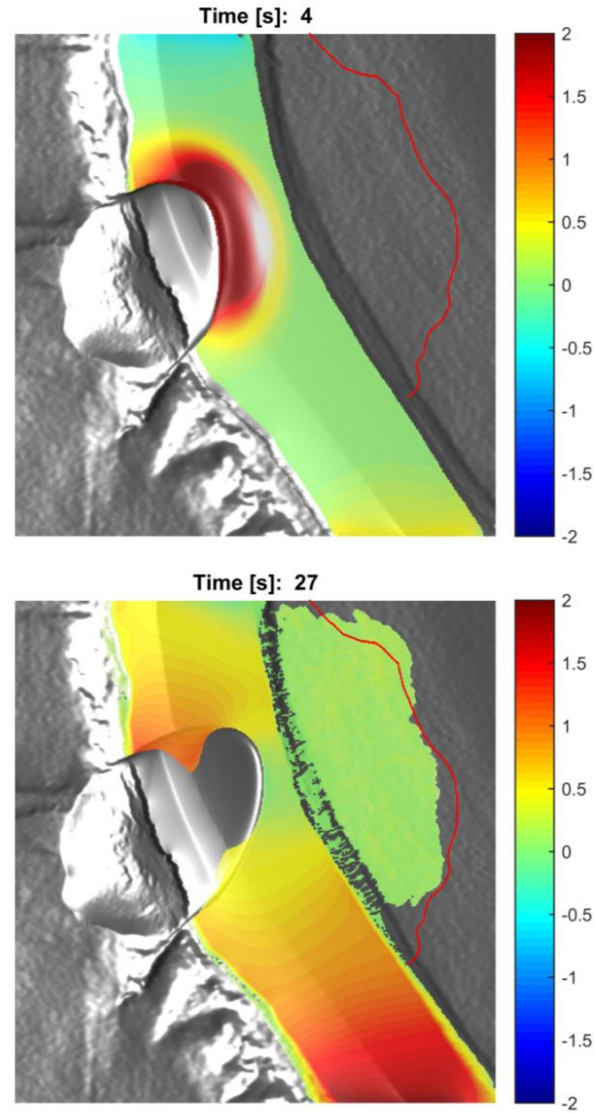

Figure 4. 2.5D simulation results. Red line: Real extension of the run-up. Top: Generation of the wave by the landslide pushing the water. Bottom: The simulated run-up reaches its maximum extension.

5 DISCUSSION

The 1D model simulates a realistic propagation distance. The slightly too long distance (~10 m) can be explained by the fact that intrinsically with a 1D model, the mass of water cannot be spread laterally (in the second dimension).

Concerning the 2.5D model, even if the simulation doesn't fit perfectly the real extension, the model is considered as relevant. Moreover, the difference could not only be imputed to the tsunami model but also to the inputs. Indeed, as mentioned previously, the bathymetry has been numerically constructed and certainly differs from the true one. On the other hand, the landslide is also implemented as an input and its numerical behavior does not reflect the real behavior. Also, the movement and the spreading of the slide were very probably affected by the flow of the river, meaning that it should have changed its trajectory over time.

As it has been also discussed by Locat et al. (2015, this volume) the slide mechanics here is such that most of the movement is in the horizontal direction. In this way the slide acts like a piston resulting in a directionality which is far more significant than when a slide falls a in a body of water where more radiation takes place (e.g. Leblanc et al. 2015, this volume). Such a condition is believed to be frequent for slides in quick clays and the model presented here provides another alternative to study the impact of such phenomena.

6 CONCLUSION

This paper shows that our model is able to simulate quite precisely the tsunami generated by the Nicolet landslide that occurred in May 2006. This observations together with numerical tests detailed in Franz et al., 2013 and comparison with others models lead us to consider our model as valid and as a relevant tool for tsunami modeling and for the assessment of the associated risks. Especially as this case study combines supplementary difficulties such as the river flow.

7 PROSPECTS

Some differences between the result of the model and the field observation are due to the assumption made on the unknown geometry of the river bed. In order to reduce these uncertainties, field work are planned to measure the bathymetry. Also, different models of landslide propagation will be tested and used as input for the tsunami model.

The Lax-Friedrichs scheme is generally known to be to diffusive. This issue is not to present in this case study thanks to the high resolution of the DEM, nevertheless, an even increased resolution could help to reach more accurate results.

8 ACKNOLEDGMENTS

The authors would like to acknowledge the Ministère des Transports du Québec for providing the ALS and the TLS data on the Nicolet landslide.

9 REFERENCES

Franz, M., Podladchikov, Y., Jaboyedoff, M. and Derron, M-H. 2013. Landslide-triggered tsunami modelling in alpine lakes. *International Conference Vajont 1963-2013. Thoughts and analyses after 50 years since the catastrophic landslide*. Italian Journal of Engineering Geology and Environment – Book Series (6) Padua, Italy

Heller, V., Hager, W.H., and Minor, H.-E. 2009. Landslide generated impulse waves in reservoirs: Basics and computation. *Mitteilungen 211, VAW*, R. Boes, Hrsg., ETH Zürich.

Jaboyedoff, M., Baillifard, F., Couture, R., Locat, J. and Locat, P. 2004. Toward preliminary hazard assessment using DEM topographic analysis and simple mechanical modeling by means of sloping local base level. In: Lacerda, Ehrlich, Fontoura and Sayao (2004, eds.). *Landslides: Evaluation and Stabilisation*. Taylor & Francis Groupe, London.

Jaboyedoff, M., Demers, D., Locat, J., Locat, A., Locat, P., Oppikofer, T., Robitaille, D. and Turmel, D. 2009. Use of terrestrial laser scanning for the characterization of retrogressive landslides in sensitive clay and rotational landslides in river banks. *Canadian Geotechnical Journal*, 46: 1379-1390.

Kremer, K., Simpson, G. and Girardclos, S. 2012. Giant Lake Geneva tsunami in ad 563. *Nature Geoscience* 5: 756-757.

Løvholt, F., Glimsdal, S., Lynett, P. and Pedersen, G. 2015. Simulating tsunami propagation in fjords with long-wave models. *Nat. Hazards Earth Syst*. Sci, 15, 657-669.

Minoia, R. and Oppikofer, T. 2006. Mesure au Scanner Laser 3D du glissement de terrain de Nicolet. *Report UNIL-IGAR.*

Slingerland R.L. & Voight B. 1979. Occurrences, properties, and predictive models of Landslide-generated water waves. In: Voight B. (1979, eds.) – *Rockslide and avalanches*, vol. 2: 317-397, Elsevier, Amsterdam.

Toro, E.F. 2001. *Shock-Capturing Methods for Free-Surface Shallow Flows*. Wiley, New York.

Toro, E.F. and Garcia-Navarro, P. 2010. Godunov-type methods for free-surface shallow flows: A review. *Journal of Hydraulic Research*, 45: 736-751.

Turcotte, D.L. and Schubert, G. 2002. *Geodinamics*. Cambridge University Press.

Ward, S.N. and Day, S. 2011. The 1963 Landslide and Flood at Vajont Reservoir Italy. A tsunami ball simulation. *Ital.J.Geosci*., 130: 16-26.

Wieczorek, G.F., Geist, E.L., Motyka, R.J. and Jakob, M. 2007. Hazard assessment of the Tidal Inlet landslide and potential subsequent tsunami, Glacier Bay National Park, Alaska. *Landslides*.

Zijlema, M. and Stelling, G.S. 2008. Efficient computation of surf zone waves using nonlinear shallow water equations with non-hydrostatic pressure. *Costal Engineering, 55: 780-790.*